PHYSICAL REVIEW B VOLUME 23, NUMBER 2 15 JANUARY 1981

Self-consistent charge densities, band structures, and staging energies of graphite intercalation compounds

S. A. Safran* and D. R. Hamann
Bell Laboratories, Murray Hill, New Jersey 07974
(Received 30 July 1980)

A model, self-consistent band structure is calculated for a thin film of n graphite layers bounded by two, partially ionized intercalant layers for stages $n = 2$–8. The quantum mechanics of the electrons in the graphite layers is modeled using a variant of the three-dimensional linear combination of atomic orbitals Hamiltonian whose parameters have been determined for pure graphite. The effects of the nonhomogeneous distribution of electrons in the n layers (screening) are taken into account by adding a *self-consistently determined* layer-potential term to the tight-binding Hamiltonian. The layer charge densities, potentials, and total energies are presented for $n = 2$–8 along with representative band structures for charge transfer per intercalant (f) of $f = 1$ and 1/4 (referred to $C_{12n}X$). The stage dependence of the total energy in this model is related to the stage dependence of the chemical potential (intercalant vapor pressure) in an intercalation reaction. Comparison of theory and experiment indicates the significance of the electronic energy in stabilizing the high-stage structures.

INTRODUCTION

The existence of stage ordering in graphite intercalation compounds[1-3] (a c-axis superlattice of a sequence of n graphite layers and one intercalant layer) has motivated many[1-3] studies of the stage dependence of both the lattice and electronic properties of these materials. In addition, recent efforts have also been directed towards a fundamental understanding of the underlying mechanisms[4,5] and long-range interactions that give rise to the high ($n \sim 10$) stages observed in *some*[6] materials. Since the sequence of stages constitutes a particularly simple class of one-dimensionally modulated structures (almost unique to intercalated graphite) an understanding of the origin, phase diagrams,[7] and effects of staging is of general interest as well.[8-10] This paper focuses on the effects of staging on the electronic structure of graphite intercalation compounds, through a self-consistent, model band-structure calculation. Particular emphasis is placed on the role of the unusual nature of the c-axis screening in determining the nonhomogeneous charge distribution. Theoretical studies[11,12] based on (semiclassical) Thomas-Fermi theory have shown that the screening (and resulting contribution to the energy) of the intercalant layers by the charges donated to the graphite is long-ranged (nonexponential), so that the nature of the screening in a full *quantum* treatment is of intrinsic interest. Finally, total energy calculations are presented, which indicate the role of the electronic energy in stabilizing the ordered high-stage structures. Our results for this quantum-mechanical treatment are compared to those obtained from a Thomas-Fermi[12] calculation.

The stage dependence of the electronic properties of graphite intercalation compounds has been studied using both Fermi surface (e.g., de Haas–van Alphen[13-15] effect, magnetoreflection,[16] magneto-oscillations[17,18]) and full band (e.g., optical properties,[19,20] electron spectroscopy[21,22]) probes. Although first-principles band-structure calculations have been performed for the stage-one compounds C_8K and C_6Li, the prospects of performing them for high-stage materials are slim. Several model band structures, all based upon electrons propagating in (modified) graphite bands have recently been proposed. In these calculations, the hybridization of the carbon and intercalant orbitals is ignored and a parameter f is introduced to define the change transfer per intercalant to the carbon atoms. Holzwarth[23] has pointed out that a completely "rigid-band"[14,24] approach based upon the mere raising (or lowering) of the Fermi level of three-dimensional graphite is inappropriate, since the discrete c-axis quantization of a small number of graphite layers is quite different from the c-axis dispersion of prinstine graphite. Dresselhaus *et al.*[13] have calculated a model band structure for stage-n compounds taking into account the changes due to the existence of n layers in the unit cell. However, their treatment ignores the long-range Coulomb interactions which give rise to screening. Blinowski *et al.*[19] have demonstrated the importance of including these electrostatic effects in a calculation of band structures for stages three (self-consistent) and four (non-self-consistent) using a simplified tight-binding model which they treat analytically. In the present work, we present a self-consistent calculation of the band structures, layer potentials, charge

densities, and total energies for stages $n=2-8$ using the *full* tight-binding Hamiltonian as discussed in Ref. 23, but with the long-range Coulomb interactions included. The potential is self-consistently determined to $0.002-10^{-6}$ eV (per carbon atom) and all quantities are calculated from full-zone integrations. We show how the Coulomb terms, which can result in large (~0.25 eV) changes in the electronic energy levels are crucial for a physically reasonable screening charge density. The proper treatment of the self-consistent potential is also necessary for calculations of the stage dependence of the total energy. It is the *decrease* in total energy as the stage *increases*, that stabilizes the staged structures and that determines the stage dependence of the chemical potential of the intercalant in the intercalation process. (A preliminary report of this work was presented in Ref. 5.)

In Sec. I, we present the tight-binding Hamiltonian including the self-consistent potential. Our Hamiltonian is compared to that of Refs. 23, 13, and 25 and the convergence criteria for self-consistency are discussed. Section II contains our results for the layer potentials and charge densities for stages 2–8 and charge transfers $f=1$ and $\frac{1}{4}$ (referred to a $C_{12n}X$ compound). The results of the total energy calculations are presented in Sec. III where the range of stability[5,7] of a given stage as a function of the chemical potential (for intercalant atoms) is also calculated. In Sec. IV we summarize our results and relate them to experiment.

I. MODEL HAMILTONIAN

In this section, we derive our model Hamiltonian from an expression for the total energy of n graphite layers bounded by two intercalant layers. Because of the periodicity of the staged structure, each intercalant atom in the corresponding thin-film model has charge $f/2$, where f is the charge transfer per intercalant for the periodic, staged compound. Although our calculations are presented for donor compounds ($f>0$) the same qualitative results occur for acceptor ($f<0$) compounds.

The main assumptions of our model are the following:

(i) The hybridization between the graphite and intercalant orbitals is negligible, so that an effective charge transfer per intercalant (f) of electrons to the π bands of graphite can be defined.

(ii) The quantum mechanics of the electrons in the graphite layers is described by a linear combination of atomic orbitals (LCAO) graphite π-band Hamiltonian (suitably modified to describe the thin film). Changes in the tight-binding *parameters* due to charge transfer are neglected.

(iii) The *in-plane* spatial *variations* of the electrostatic potential due to the charged intercalant and graphite layers are neglected. Thus, as far as the electrostatics are concerned, both the graphite and the intercalant layers are treated as charged sheets with an inhomogeneous potential along the c axis only.

(iv) Hopping between graphite layers separated (5–9 Å) by an intercalant layer is neglected as is hopping between *next*-nearest-neighbor graphite layers. Thus, the n-layer sandwiches in a stage-n material are decoupled and the problem reduces to that of the thin film.

Assumption (i) has been justified in first-principles calculations of the band structures of the stage-one compounds[26-28] C_8K and C_6Li, where the bands near the Fermi energy are well described by an LCAO or tight-binding model. Blinowski[19] has shown that (ii) and (iii) are reasonable assumptions and typically lead to small corrections. [In general, one can show from Poisson's equation that corrections to (iii) lead to exponentially small terms of the form e^{-Gz}, where G is the smallest in-plane reciprocal-lattice vector.] The justification for assumption (iv) is that second-layer LCAO matrix elements (γ_2,γ_5) in graphite are ~0.02 eV.[23,25] Since the bandwidth due to in-plane dispersion is ~9 eV and because the range of both first-layer LCAO matrix elements and the electrostatic potential are several tenths of an eV, second-layer hopping can be neglected in the intercalation compounds. Of course, in pristine graphite, nonzero values for the second-layer matrix elements are crucial for obtaining semimetallic behavior. However, since pure graphite has only 10^{-4} electrons per carbon, while the intercalation compounds result in $10^{-1}-10^{-3}$ electrons per carbon, the small energies due to γ_2 and γ_5 can be neglected, at least for stages 2–8 considered here. Furthermore, corrections due to assumptions (i)–(iii) are expected to yield changes of this (~0.02 eV) order.

With these approximations, the total energy per carbon atom (U_n) of the n-graphite layers and the two intercalant layers can be written

$$U_n=\langle H_0\rangle+U_{ee}+U_{ei}+U_{ii}. \tag{1}$$

In Eq. (1), H_0 is the Hamiltonian describing the n-graphite layers (without any Coulomb terms due to charge transfer). U_{ee}, U_{ei}, and U_{ii} are the Coulomb energies of interaction among the *charged* graphite layers, the graphite and intercalant layers and the two intercalant layers. (The charges are referred to *neutral* graphite layers.) The

exact wave functions of the interacting system are written $\psi_p^{\vec{k}}(\vec{r})$, where $\vec{k}$ is a two-dimensional (in-plane) wave vector defined in the Brillouin zone shown in Fig. 1, and p is a band index ($p=1,\ldots,2n$ for stage n with only the π orbitals considered). The wave function $\psi_p^{\vec{k}}(\vec{r})$ is expanded in a basis of orthonormal orbitals (e.g., Wannier functions) $\phi(\vec{r}-\vec{R}_{\alpha i})$ localized on the carbon atom in layer i ($i=1,\ldots,n$). The index $\alpha=a,b$ denotes the two atoms in the unit cell of a single graphite layer (see Fig. 1). Thus,

$$\psi_p^{\vec{k}}(\vec{r})=\sum_{\alpha i} c_{pi}^{k\alpha} e^{-i\vec{k}\cdot\vec{R}_{\alpha i}}\phi(\vec{r}-\vec{R}_{\alpha i})\,, \tag{2a}$$

$$\langle\phi(\vec{r}-\vec{R}_{\alpha i})|\,\phi(\vec{r}-\vec{R}_{\beta j})\rangle=\delta_{i,j}\delta_{\alpha,\beta}\,. \tag{2b}$$

Using this notation, $\langle H_0\rangle$ can be written

$$\langle H_0\rangle=\frac{1}{n}\sum_{pk} f_p^k\langle\psi_p^{\vec{k}}|H_0|\psi_p^{\vec{k}}\rangle$$
$$=\frac{1}{n}\sum_{pk}\sum_{\alpha\beta,ij} f_p^k c_{pi}^{k\alpha *} c_{pj}^{k\beta} E_{\alpha\beta}^{ij}(\vec{k})\,. \tag{3}$$

In Eq. (3) f_p^k is a weight factor composed of the product of an energy normalization factor w_k and a Fermi function $\{\exp\beta[\epsilon_p(\vec{k})-\epsilon_F]+1\}^{-1}$, where $\beta=1/k_BT$, $\epsilon_p(\vec{k})$ is the energy corresponding to $\psi_p^{\vec{k}}(\vec{r})$, and ϵ_F is the Fermi energy. The energy normalization factor is chosen so that U_n is the energy per carbon atom in the n-layer sandwich. The normalization also includes the factor of two to account for the spin so $(1/n)\sum_{pk} w_k=2$, the maximum number of π electrons per carbon atom. The matrix $E_{\alpha\beta}^{ij}(\vec{k})$, is given in Appendix A and is similar to the matrix $H_{ab}^{ij}(\vec{k})$, etc., defined by Holzwarth.[23] $E_{\alpha\beta}^{ij}(\vec{k})$ is the LCAO matrix that describes the quantum mechanics (both the in-plane and interplanar) using localized graphite orbitals. A simplified version of $E_{\alpha\beta}^{ij}(\vec{k})$ for stages $n=3,4$ is given in Ref. (19). Note that $E_{\alpha\beta}^{ij}(\vec{k})$ is equivalent to the Hamiltonian of Dresselhaus *et al.*[13] if second-layer interactions are set equal to zero [see assumption (iv) above].

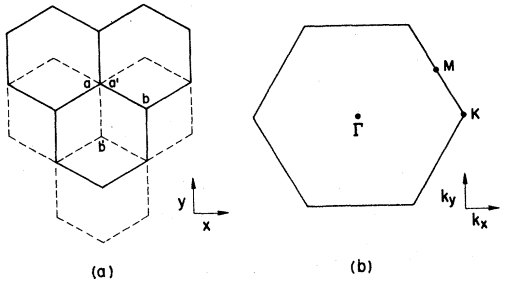

FIG. 1. (a) Real space lattice for graphite layers in "*AB* stacking." The solid line is the *A* layer and the dashed line is the *B* layer displaced along the *c* axis by c_0. The two atoms in the unit cell are shown for the *A* (unprimed) and *B* layers. (b) Two-dimensional Brillouin zone for a single graphite layer. The symmetry points Γ, K, and M are located at $(0,0)$, $(2\pi/a)(\frac{2}{3},0)$, and $(2\pi/a)(\frac{1}{2},1/2\sqrt{3})$, respectively, where a is the graphite in-plane lattice constant.

In the charged sheet [see assumption (iii) above] approximation,

$$U_{ee}=\frac{-V_0}{2n}\sum_{ij} q_i q_j|i-j|\,, \tag{4a}$$

$$U_{ei}=\frac{V_0}{n}\frac{\tilde{f}}{2}[(n-1)+2\eta]\sum_i q_i\,, \tag{4b}$$

$$U_{ii}=\frac{-V_0}{n}\frac{\tilde{f}^2}{4}[(n-1)+2\eta]\,. \tag{4c}$$

In Eq. (4) n is the stage or the number of graphite layers in the thin film, q_i is the average charge per carbon atom in the ith layer ($i=1,\ldots,n$) and $\tilde{f}/n$ is the average charge transfer per carbon atom in the n layers so that $\sum_i q_i=\tilde{f}$. The energies U_{ee}, U_{ei}, and U_{ii} are per carbon atom, and the energy scale V_0 is given by

$$V_0=2\pi\sigma_0 e^2 c_0/\epsilon\,, \tag{5}$$

where σ_0 is the areal density of carbon atoms, c_0 is the c-axis separation of two carbon layers ($c_0=3.35$ Å), and ϵ is an appropriate dielectric constant (for an electric field $\vec{E}\|\vec{c}$) that describes the screening by the graphite σ electrons. Appendix B presents a discussion of the dielectric constant ϵ; in our calculations, we used values of $\epsilon=2$ and 3 as lower and upper bounds, respectively (see Appendix B). The parameter η in Eq. (4) is the ratio of the carbon–intercalant to carbon–carbon distance. The quantity η does not enter into the self-consistent band equations. It also does not affect the range of stability of the chemical potential, discussed in Sec. III, and is merely an additive constant to the total energy of the n layers.

Since the average charge of n carbon atoms (relative to pure graphite) in the n carbon layers is

$$\tilde{f}=\sum_{pk} f_p^k\langle\psi_p^{\vec{k}}|\,\psi_p^{\vec{k}}\rangle-n \tag{6a}$$

$$=\sum_{pk,\alpha i} f_p^k|\,c_{pi}^{k\alpha}|^2-n\,. \tag{6b}$$

We identify q_i with

$$q_i=\sum_{pk,\alpha} f_p^k|\,c_{pi}^{k\alpha}|^2-1\,. \tag{6c}$$

The energy per carbon atom can then be rewritten using Eqs. (1), (3b), (4), and (6c) as (note that $U_{ei}+U_{ii}=-U_{ii}$)

$$U_n=\frac{1}{n}\left[\sum_{p\vec{k}} f_p^{\vec{k}} \sum_{ij,\alpha\beta} c_{pi}^{k\alpha *} c_{pj}^{k\beta} E_{\alpha\beta}^{ij}(\vec{k}) - \frac{V_0}{2}\sum_{ij}|i-j|\left(\sum_{p\vec{k},\alpha} f_p^{\vec{k}}|c_{pi}^{k\alpha}|^2-1\right)\left(\sum_{p'\vec{k}',\beta} f_{p'}^{\vec{k}'}|c_{p'j}^{k'\beta}|^2-1\right)\right]-U_{ii}\,.$$

The coefficients $\{c_{pi}^{k\alpha}\}$ are determined by the minimization of U with respect to the $c_{pi}^{k\alpha}$ with the constraint that the $\{\psi_p^{\vec{k}}(\vec{r})\}$ be orthonormal. These conditions yield

$$\sum_{\beta j}[E_{\alpha\beta}^{ij}(\vec{k})+\tilde{V}_i\delta_{\alpha\beta}\delta_{ij}]c_{pj}^{k\beta}=\epsilon_p(\vec{k})c_{pi}^{k\alpha}\,, \tag{8}$$

where $\tilde{V}_i$ is the self-consistent potential at layer i due to the other charged layers

$$\tilde{V}_i=-V_0\sum_j q_j|i-j|\,, \tag{9}$$

with the $\{q_i\}$ related to the $\{c_{pi}^{k\alpha}\}$ by Eq. (6c). With a starting guess for the $\{q_i\}$ and hence the $\{\tilde{V}_i\}$, Eq. (8) is diagonalized and the eigenvalues $\{\epsilon_p(\vec{k})\}$ and the eigenvectors $\{c_{pi}^{k\alpha}\}$ are determined. After determining the Fermi energy, ϵ_F and the weights $f_p^{\vec{k}}$, the new charge distribution $\{q_i\}$ and the potential $\{\tilde{V}_i\}$ are recomputed. The process is iterated to consistency, and for our calculations we require the input and output layer potentials $\{\tilde{V}_i\}$ to differ by less than 0.002 eV.

The final expression for the energy U_n is obtained by multiplying Eq. (8) by $c_{pi}^{k\alpha *}$, comparing to Eq. (7), and using $\sum_{\alpha i}|c_{pi}^{k\alpha}|^2=1$ (orthonormality) to find that

$$U_n=\frac{1}{n}\left[\sum_{p\vec{k}} f_p^{\vec{k}}\epsilon_p(\vec{k})-\sum_i\left(\frac{q_i}{2}+1\right)\tilde{V}_i\right]-U_{ii}\,, \tag{10}$$

where q_i and $\tilde{V}_i$ are determined by the self-consistent solution for the $\{c_{pi}^{k\alpha}\}$ using Eqs. (6c) and (9), and U_{ii} is given by Eq. (4c).

Equations (6c), (9), (8), and (10) are the main results of this section for determining the charge and potential distributions among the layers, eigenvalues, and wave functions, and total energies per carbon atom, respectively. The self-consistent numerical solutions of these equations are discussed in Sec. II.

II. ENERGY BANDS, LAYER POTENTIALS, AND CHARGE DENSITIES

This section presents the solutions of Eqs. (8), (9), and (6c) for the energy bands, and the potential and charge distributions, for the model described in Sec. I. The results are contrasted with those of a non-self-consistent rigid-band solution of Eq. (8) (i.e., $\{\tilde{V}_i\}=0$) to demonstrate the importance of including the Coulomb terms $\{\tilde{V}_i\}$.

The self-consistent solution of Eqs. (6c), (8), and (9) is straightforward. The LCAO parameters which enter the matrix $E_{\alpha\beta}^{ij}(\vec{k})$ are discussed and given in Appendix A. Values of $\epsilon=2$ and $\epsilon=3$ were used for the effective diectric constant ϵ [Eq. (5)] as discussed in Appendix B. Self-consistency was assumed to be reached when the input and output layer potentials $\{V_i\}$ differed by 10^{-6} eV per carbon atom in *each layer*. (The calculations for the charge densities for $\epsilon=2$ are self-consistent to 0.002 eV.) Integrations were performed over a coarse mesh of ~650 equally spaced[29] points for the *full* irreducible wedge of the two-dimensional Brillouin zone, and an additional fine mesh of ~300 points was used in a small region of the Brillouin zone near the $K[\vec{k}=2\pi/a(\frac{2}{3},0)]$ point.

Figure 2 shows representative energy bands for $n=5$. In Fig. 2(b), the bands for $\tilde{f}=\frac{1}{12}$ (corresponding to a charge transfer per intercalant $f=1$ referred to a $C_{12n}X$ compound) and a value of $\epsilon=3$ are shown. The lower-energy conduction bands have wave functions mostly localized in the bounding graphite layers, while the highest-lying bands have wave functions mostly localized in the interior graphite layers. Figure 2(a) shows the same bands ($\tilde{f}=\frac{1}{12}$) for a value of $\epsilon\to\infty$ or $\{\tilde{V}_i\}\equiv 0$, corresponding to a rigid-band, non-self-consistent solution of the n-layer LCAO Hamiltonian. Note the large (~0.25 eV) changes in the band structure which result from the self-consistent potential. These changes are less significant for smaller values of the charge transfer as shown in Fig. 2(c) where the energy bands for $n=5$, $\tilde{f}=\frac{1}{48}$ (corresponding to $f=\frac{1}{4}$ for $C_{12n}X$), and $\epsilon=3$ are shown. The energy bands for the smaller value of $\epsilon=2$ are similar to those for $\epsilon=3$ with the effects of the potential and the modifications of the rigid-band even larger.

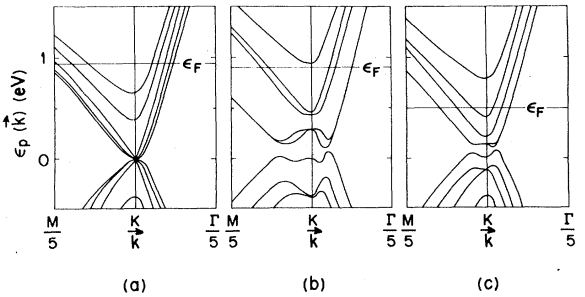

FIG. 2. Energy bands $[\epsilon_p(\vec{k})]$ for stage $n=5$. ϵ_F is the Fermi energy and the Γ, K, and M points are defined in Fig. 1(b). (a) $\tilde{f}=\frac{1}{12}$ (charge transfer per intercalant $f=1$ for $C_{12n}X$) non-self-consistent ($\epsilon\to\infty$, $\{V_i\}=0$) results. (b) $\tilde{f}=\frac{1}{12}$ ($f=1$ for $C_{12n}X$) self-consistent calculation $\epsilon=3$. (c) $\tilde{f}=\frac{1}{48}$ ($f=\frac{1}{4}$ for $C_{12n}X$) self-consistent calculation $\epsilon=3$.

TABLE I. c-axis charge distribution $\{q_i\}$ stage $n=8$; $f=1$[a]; $\tilde{f}=\frac{1}{12}$[b] (units: electrons per carbon atom).

Layer[c]	Self-consistent bands $\epsilon=3$	Self-consistent bands $\epsilon=2$	Non-self-consistent	Thomas-Fermi ($\epsilon=3.4$)[d]
1	0.0325	0.0347	0.0106	0.0327
2	0.0058	0.0047	0.0103	0.0058
3	0.0022	0.0015	0.0104	0.0020
4	0.0012	0.0007	0.0104	0.0011

[a] f is the charge transfer per intercalant atom, here referred to a $C_{12n}X$ compound.

[b] $\tilde{f}/n$ is the average charge transfer per carbon atom in the n layers so that $\sum_i q_i=\tilde{f}$.

[c] Layers are labeled consecutively with layer 1 being the graphite layer adjacent to the intercalant (bounding layer).

[d] See Appendix B for a discussion of the different dielectric constants. (The agreement for smaller values of f is not quite as good since for small f, interlayer hopping, neglected in the Thomas-Fermi treatment, is more important.)

Although the electronic energy bands are one indication of the importance of the potential $\{\tilde{V}_i\}$, a quantity that is much more sensitive to the potential is the layer charge per carbon atom $\{q_i\}$.

Table I compares the layer charges for $n=8$ and $\tilde{f}=\frac{1}{12}$ ($f=1$ for $C_{12n}X$) obtained from the self-consistent and non-self-consistent ($\{\tilde{V}_i\}=0$) calculations. Also shown are the layer charges obtained by integrating the continuum charge density of the Thomas-Fermi[11,12,30] model, around each layer. The self-consistent solution for $\{q_i\}$ shows the effects of the screening in good agreement with the simple Thomas-Fermi results,[11,12,30] which neglect[30] c-axis hopping. On the other hand, the neglect of the layer potentials $\{\tilde{V}_i\}$ ($\epsilon\to\infty$) results in an almost uniform charge density. Also shown in Table I are results for $\epsilon=2$ which show how the charge distribution is *less* homogeneous for smaller values of ϵ (Ref. 11) for both the Thomas-Fermi and band calculations. For all cases, the band calculation results in a *more* homogeneous charge distribution than does the Thomas-Fermi model. This is probably due to the effects of c-axis hopping.

Complete results for stages $n=2$–8 for values of $\tilde{f}=\frac{1}{12}$ and $\frac{1}{48}$ ($f=1$ and $\frac{1}{4}$ for $C_{12n}X$) are shown in Tables II and III for values of $\epsilon=3$ and 2, respectively. Along with the layer charges per carbon atom, we also list the layer potentials, with the bounding graphite layer (i.e., the graphite layer

TABLE II. Layer potentials and c-axis charge distributions (self-consistent bands $\epsilon=3$).

Layer[b]	$\tilde{f}=\frac{1}{12}$[a] Charge (per carbon)	$\tilde{f}=\frac{1}{12}$[a] Potential[c] (eV)	$\tilde{f}=\frac{1}{48}$[a] Charge (per carbon)	$\tilde{f}=\frac{1}{48}$[a] Potential[c] (eV)
($n=3$)				
1	0.0353	0.0	0.0083	0.0
2	0.0128	0.494	0.0043	0.165
($n=4$)				
1	0.0335	0.0	0.0074	0.0
2	0.0082	0.628	0.0031	0.236
($n=5$)				
1	0.0329	0.0	0.0070	0.0
2	0.0068	0.672	0.0024	0.262
3	0.0039	0.822	0.0020	0.337
($n=6$)				
1	0.0326	0.0	0.0069	0.0
2	0.0062	0.702	0.0022	0.274
3	0.0029	0.925	0.0014	0.380
($n=7$)				
1	0.0326	0.0	0.0068	0.0
2	0.0060	0.701	0.0022	0.277
3	0.0023	0.943	0.0011	0.388
4	0.0017	1.010	0.0007	0.415
($n=8$)				
1	0.0325	0.0	0.0067	0.0
2	0.0058	0.705	0.0020	0.284
3	0.0022	0.963	0.0010	0.414
4	0.0012	1.055	0.0007	0.466

[a] See Table I, Refs. a and b.

[b] See Table I, Ref. c.

[c] Potential is relative to bounding graphite layer (layer 1).

TABLE III. Layer potentials and c-axis charge distribution (self-consistent bands $\epsilon = 2$).

Layer[b]	$\tilde{f} = \frac{1}{12}$[a] Charge (per carbon)	$\tilde{f} = \frac{1}{12}$[a] Potential[c] (eV)	$\tilde{f} = \frac{1}{48}$[a] Charge (per carbon)	$\tilde{f} = \frac{1}{48}$[a] Potential[c] (eV)
($n=3$)				
1	0.0365	0.0	0.0086	0.0
2	0.0104	0.597	0.0037	0.209
($n=4$)				
1	0.0354	0.0	0.0079	0.0
2	0.0063	0.731	0.0025	0.288
($n=5$)				
1	0.0349	0.0	0.0077	0.0
2	0.0054	0.788	0.0020	0.317
3	0.0028	0.951	0.0014	0.396
($n=6$)				
1	0.0348	0.0	0.0076	0.0
2	0.0049	0.799	0.0019	0.330
3	0.0020	1.024	0.0009	0.438
($n=7$)				
1	0.0346	0.0	0.0075	0.0
2	0.0049	0.819	0.0018	0.339
3	0.0017	1.074	0.0008	0.466
4	0.0011	1.136	0.0006	0.496
($n=8$)				
1	0.0347	0.0	0.0075	0.0
2	0.0047	0.822	0.0018	0.345
3	0.0015	1.086	0.0007	0.483
4	0.0007	1.170	0.0005	0.537

[a] See Table I, Refs. a and b.
[b] See Table I, Ref. c.
[c] Potential is relative to bounding graphite layer (layer 1).

adjacent to the intercalate potential set equal to zero. The potential differences between the layers are as large as ~0.7 eV between the bounding and its nearest graphite layer. While the potential differences between the interior-most layers are smaller, especially for small values of $\tilde{f}$, it is not clear *a priori* that they can be neglected in a general band-structure calculation.

III. STAGING ENERGIES: STABILITY OF PURE STAGES

This section presents the results of our calculations of the total energy for the "thin-film" model discussed above. The role of the electronic energy in stabilizing the stage ordering is then demonstrated in a calculation of the stage dependence of the chemical potential. For discussions of *elastic* interactions and staging in graphite intercalation compounds, see Refs. 4 and 12.

In this section, we assume for computational convenience, that the sequence of stages is described by the chemical formula $C_{tn}X$, where $n=1, 2, \ldots$ describes the stage, and t is stage independent. Assuming that all interlayer intercalant-intercalant interactions are electronic in origin, we write the total energy for the intercalant, $\overline{E}_n$, as

$$\overline{E}_n = -\frac{\mu}{n} + t(U_n - U_\infty) . \tag{11}$$

In Eq. (11) U_n is given by Eq. (10) and μ is the chemical potential for the intercalant atoms. Since the zero of energy is arbitrary, μ is defined to include all *stage-independent* energies, such as the energy of the intercalant layer due to *in-plane* intercalant-intercalant interactions. U_∞ is the energy per carbon atom of pristine, bulk graphite, so that $\overline{E}_n$ reflects only the effects of intercalation. Thus, although Eq. (11) cannot predict the dependence of μ on the in-plane intercalant density, it does describe the stage dependence of μ for constant in-plane intercalant density (i.e., t independent of n).

At zero-temperature, the transitions between stages are first order,[5,7] and the phase boundary ($\mu_{n,n'}$) between stages n and n' is given by

$$\mu_{n,n'} = t\left(\frac{U_n - U_{n'}}{n^{-1} - n'^{-1}}\right). \tag{12}$$

Equation (12) is obtained from Eq. (11) by equating the energies $\bar{E}_n$ for stages n and n' at $\mu = \mu_{n,n'}$. (At each phase boundary one must check to make sure that no other stage has lower energy.) Assuming a simple sequence of stages $1, 2, \ldots$ as μ is lowered ($\mu_{n,n'} = \mu_{n,n\pm1}$), the range of stability of a given stage is defined by $\Delta\mu_n$, where

$$\Delta\mu_n \equiv \mu_{n,n-1} - \mu_{n,n+1} . \tag{13}$$

Writing the electronic energy per intercalant $E_n \equiv tnU_n$, we have[5,7,12]

$$\Delta\mu_n = n(E_{n+1} + E_{n-1} - 2E_n). \tag{14}$$

Thus, the range of chemical potential over which a given stage is stable ($\Delta\mu_n$) is an important experimental parameter since it is directly related to the interlayer interactions responsible for staging. For the Thomas-Fermi model of the total energy[12]

$$E_n = E_0\left[1 + \alpha\left(1 + \frac{n}{n_0}\right)^{-5}\right], \tag{15}$$

where $\alpha = 0.96$. For $C_{12n}X$ with unit charge transfer ($f = 1$, $\tilde{f} = \frac{1}{12}$) and for a dielectric constant $\epsilon = 3.4$ (see Sec. II and Appendix B), $E_0 = 1.26$ eV and $n_0 = 2.98$.

The Thomas-Fermi result for the stage dependence of the chemical potential is shown in Fig. 3 along with results for the self-consistent calculation described above ($\tilde{f} = \frac{1}{12}, \epsilon = 3$). Since the quantity that determines $\Delta\mu_n$ is the energy per *intercalant* it was necessary to calculate the layer potentials to self-consistency within 10^{-6} eV to get energy resolution (per intercalant) of ~0.001 eV.

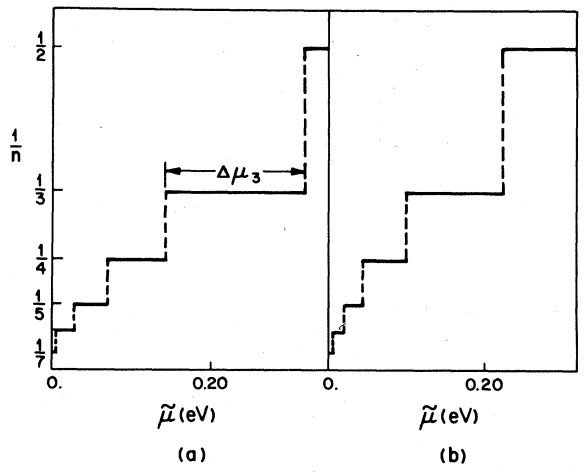

FIG. 3. Stage dependence of the chemical potential $\tilde{\mu}$ defined in the text ($\tilde{f} = \frac{1}{2}$; $f = 1$ for $C_{12n}X$). (a) Self-consistent band calculation ($\epsilon = 3$). (b) Continuum Thomas-Fermi model ($\epsilon = 3.4$, see Appendix B). The physical quantity of importance is $\Delta\mu_n \equiv \mu_{n,n-1} - \mu_{n,n+1}$.

In Fig. 3, we plot $\tilde{\mu} = \mu - \mu_0$, where μ_0 is an arbitrary zero of energy, chosen so that $\tilde{\mu}_{7,8} = 0$. In Sec. IV, values for $\Delta\mu_n$ are compared with experiment. Here we note that although there is good agreement between the Thomas-Fermi model and the self-consistent bands, with respect to the charge distribution (see Table I), the differences in $\Delta\mu_n$ are more severe. The fact that the band calculation results in larger values of $\Delta\mu_n$ is probably due to the inclusion of both interlayer hopping energies and the explicit response of the valence electrons in the thin-film calculation.

IV. DISCUSSION

The self-consistent LCAO band structure for our model of n graphite layers, bounded by two partially-ionized intercalant layers, verifies the long-range nature of the screening of the intercalant layers by the charge donated to the graphite, as predicted by the simple Thomas-Fermi model.[11,12,30] In addition, the present work results in energy bands which are quite different from those predicted by rigid-band models, and in layer potentials, which can be used in future, more realistic, calculations. The long-range (power-law) nature of the screening results in long-range, effective interactions between intercalant layers,[12] thus stabilizing the relatively high-stage structures observed in graphite intercalation compounds. An important, experimentally measurable, quantity that reflects the stability of the staged structures is the range of stability of the chemical potential ($\Delta\mu_n$) which can be calculated from our model as defined in Sec. III.

A direct comparison of the theoretical and experimental values for $\Delta\mu_n$ is difficult since neither the exact stoichiometries (and their stage dependence) nor the effective charge per intercalant f (and its stage dependence) have been determined. Nevertheless, a preliminary comparison of theoretical and experimental[31] values of $\Delta\mu_n$ for alkali-metal intercalation compounds (K, Rb, Cs, $n = 3$, 4, 5) is presented in Table IV. The theoretical calculation is for a compound with *stage-independent* stoichiometry $C_{12n}X$ and for values of $\frac{1}{4} \leq f \leq 1$. The overall agreement between theory and experiment is gratifying considering the uncertainties in the stoichiometry and charge transfer. Furthermore, the theoretical results are for low temperature, while the experiments were performed at relatively high temperatures (> 500 K),[31,32] where departures from ideal $C_{12n}X$ stoichiometry could be important as pointed out experimentally by Herold[33] and theoretically in Refs. 5 and 7. To minimize entropy effects, the experimental values of $\Delta\mu_n$ were computed from the *enthalpy* data of

Ref. 31. [The values of ΔH given in Table III of Ref. 31 are equivalent, for each two-phase equilibrium, to $(E_n - E_{n\pm1})$ of Eq. (14).] Further experiments on well-characterized samples and for high stages are clearly needed. In addition, similar thermodynamic data for acceptor compounds where the thin-film approximation should be most applicable[19] are also of interest. The agreement between theory and experiment for $\Delta\mu_n$ for the alkali metals within a factor of 2 is a good indication of the dominance of electronic interactions in the *equilibrium* staged phases (in nonequilibrium or nonhomogeneous samples, elastic interactions[5,12] become important). A further comparison of $\Delta\mu_n$ for materials with large (alkalis) and small (acceptors) values of f (see Table IV) would be a sensitive test of this mechanism.

On the theoretical front, theories for temperature effects on staging[5-7] as well as an understanding[12] of why only *pure* stage ordering has been observed are topics of current interest. Although more detailed band calculations for high-stage compounds remain to be done (including such interactions as the *in-plane* interactions between electrons and those effects of the intercalant potential that are neglected in the sheet approximation), the present calculation of self-consistent layer potentials should be useful in any future "first-principles" studies.

ACKNOWLEDGMENTS

The authors are grateful to G. Dresselhaus, N. A. W. Holzwarth, and G. Mele for stimulating discussions.

TABLE IV. $\Delta\mu_n$ $n=3,4,5$: Theory and experiment.

		$\Delta\mu_3$(eV)	$\Delta\mu_4$(eV)	$\Delta\mu_5$(eV)
Expt.[a]	$C_{12n}K$	0.095	0.026	–
	$C_{12n}Rb$	0.100	0.069	0.030(?)[b]
	$C_{12n}Cs$	0.065	0.030	0.039(?)[b]
Theory[c]	$f=\frac{1}{2}$	0.069	0.036	0.024
	$f=\frac{1}{4}$	0.029	0.019	0.007
	$f=1$	0.176	0.072	0.044

[a] See Ref. 31. The stoichiometry $C_{12n}X$ was assumed in the analysis of the data and also in the present calculation.

[b] The compound $C_{72n}X$ was not observed (Ref. 31) so the values of $\Delta\mu_5$ are hypothetical.

[c] Results are for an effective dielectric constant $\epsilon=3$. See Table I, Ref. a for definition of f.

APPENDIX A

This appendix presents an explicit expression for the LCAO Hamiltonian H_0 discussed in Sec. I. The LCAO Hamiltonian is based on the pure graphite Hamiltonian discussed in Ref. 25. The extension of that work to describe thin film of n layers was first presented in Ref. 23.

The basis for the LCAO Hamiltonian is a set of orthonormal functions (see Sec. I.) $\{\phi(\vec{r}-\vec{R}_{\alpha i})\}$, where $\alpha=a,b$ labels the two inequivalent atoms in the layer and i labels the layer. The layer geometry is shown in Fig. 1(a) where the "A" layers (solid line) are denoted as even layers 0, 2, 4 and the "B" layers (dashed line) are denoted as odd layers 1, 3, $\cdots$ in the n-layer unit cell. The matrix elements of the Hamiltonian $\langle\phi(\vec{r}-\vec{R}_{\alpha i})|H_0|\phi(\vec{r}-\vec{R}_{\beta j})\rangle$ are denoted by $E^{ij}_{\alpha\beta}$ with

$$E^{00}_{ab}=M^{010}_{ab}[e^{iak_y/\sqrt{3}}+2e^{-iak_y/2\sqrt{3}}\cos(\tfrac{1}{2}k_xa)]$$
$$+M^{0-20}_{ab}(e^{-2iak_y/\sqrt{3}}+2e^{iak_y/\sqrt{3}}\cos k_xa)$$
$$+M^{1-20}_{ab}[e^{-ik_ya/2\sqrt{3}}\cos(\tfrac{3}{2}k_xa)$$
$$+e^{-2ik_ya/\sqrt{3}}\cos k_xa$$
$$+e^{i5k_ya/2\sqrt{3}}\cos(\tfrac{1}{2}k_xa)] \quad \text{(A1)}$$

$$E^{00}_{aa}=M^{100}_{aa}\left(\cos k_xa+2\cos\frac{3ak_y}{2\sqrt{3}}\cos(\tfrac{1}{2}k_xa)\right), \quad \text{(A2)}$$

$$E^{01}_{aa}=\tfrac{3}{2}M^{001}_{aa}, \quad \text{(A3)}$$

$$E^{01}_{ab}=\tfrac{1}{2}M^{0-11}_{ab}[e^{-ik_ya/\sqrt{3}}+2\cos(\tfrac{1}{2}k_xa)e^{ik_ya/2\sqrt{3}}], \quad \text{(A4)}$$

$$E^{01}_{bb}=\tfrac{1}{2}M^{011}_{bb}[e^{ik_ya/\sqrt{3}}+2\cos(\tfrac{1}{2}k_xa)e^{-ik_ya/2\sqrt{3}}], \quad \text{(A5)}$$

$$E^{00}_{ba}=E^{00*}_{ab}, \quad \text{(A6)}$$

$$E^{00}_{bb}=E^{00}_{aa}, \quad \text{(A7)}$$

$$E^{01}_{ba}=E^{01}_{ab}. \quad \text{(A8)}$$

Note that Eq. (A7) is only approximate, consistent with our neglect of second-layer interactions, etc., which contribute energies of $\lesssim 0.02$ eV. The matrix elements corresponding to "odd" layers are

$$E^{11}_{ab}=E^{00*}_{ab}, \quad \text{(A9)}$$

$$E^{11}_{aa}=E^{00}_{aa}, \quad \text{(A10)}$$

$$E^{10}_{aa}=E^{00}_{aa}, \quad \text{(A11)}$$

$$E^{10}_{ab}=E^{01*}_{ab}, \quad \text{(A12)}$$

$$E^{10}_{ba}=E^{01*}_{ab}, \quad \text{(A13)}$$

$$E^{10}_{bb}=E^{10*}_{bb}, \quad \text{(A14)}$$

$$E_{bb}^{11}=E_{bb}^{00}, \quad \text{(A15)}$$

$$E_{ba}^{11}=E_{ab}^{00}. \quad \text{(A16)}$$

Since second-layer interactions are neglected (see Sec. I), the matrix elements for the other "even" and "odd" layers are identical to those listed for layers 0 and 1.

The coefficients $M_{\alpha\beta}^{nml}$ are defined in Ref. 23, where α, $\beta=a,b$ and $\{nml\}$ define the distance vector $\vec{t}_{nml}=na\hat{x}+(m/\sqrt{3})a\hat{y}+c_0 l\hat{z}$ between the atoms at $\vec{R}_{\alpha i}$ and $\vec{R}_{\beta j}$ (a is the in-plane lattice constant and c_0 is the interlayer distance $c_0=3.35$ Å). Values of $M_{ab}^{010}=-4.60$ eV, $M_{ab}^{0-20}=-0.74$ eV, $M_{aa}^{001}=0.25$ eV, $M_{ab}^{0-11}=0.24$ eV, and $M_{bb}^{011}=0.58$ eV were used in the present calculation (see Ref. 29 of our Ref. 23). We have neglected all matrix elements $\lesssim 0.02$ eV since changes in the LCAO matrix elements due to our approximations (see Sec. I) are of this order. Thus, we have set $M_{ab}^{1-20}=M_{aa}^{100}=0$.

APPENDIX B

This appendix discusses the effective dielectric constant relevant to our calculations. Since we treat only the π bands, the screening due to the σ and core electrons (e.g., σ-π transitions induced by the electric field $\vec{E}\|\vec{c}$), is accounted for by reducing the potenital by a factor ϵ. However, since $\pi-\pi$ transitions are implicitly *included* in our self-consistent calculations, which allow charge transfer from layer to layer for *all* the π electrons, the bulk graphite value[34-36] cannot be used without modification. We therefore need an estimate of ϵ for a single graphite layer where $\pi-\pi$ transitions are forbidden by symmetry for $\vec{E}\|\vec{c}$.

A lower bound on this effective ϵ can be obtained from atomic data, which includes all $\sigma-\pi$ transitions within a *single atom*. The polarizability of a single carbon atom has been estimated[37] to be 1.78 Å^3. From formula (A8) of Blinowski and Rigaux,[19] we find $\epsilon_{\text{atomic}}=2$.

The experimental determination of ϵ for three-dimensional graphite is not yet clear. Zanini *et al.*[35] estimate $\epsilon_{\parallel}\lesssim 3.4$, after subtracting off a Drude term for the conductivity $\lesssim 0.1$ eV. Earlier estimates in the literature indicated[34] $\epsilon_{\parallel}=2.3$ as well as[38] $\epsilon_{\parallel}=3.3$ at photon energies of $=2$ eV. The contribution of the $\pi-\pi$ transitions to these values of $\epsilon_{\parallel}$ can be estimated from the calculation of Johnson and Dresselhaus[25] for the real part of the dielectric constant for $\vec{E}\|\vec{c}$ which yields $\Delta\epsilon_{\pi\pi}=0.25$ eV. Thus the relevant value for $\epsilon=\epsilon_{\parallel}-\Delta\epsilon_{\pi\pi}$ in our calculations is in the range $2\lesssim\epsilon\lesssim 3$, with $\epsilon=2$ as a lower bound from the atomic polarizability. This range for ϵ is also consistent with the electron-energy-loss data of Venghaus[36] for energies ~5 eV where the main contribution to ϵ is from $\pi-\sigma$ transitions. We have therefore presented results for the self-consistent calculations using $\epsilon=2$ as a lower limit and $\epsilon=3$ as an upper limit. Since the Thomas-Fermi[12,30] calculations do *not* include the effects of $\pi-\pi$ transitions, they are calculated with the *full* graphite dielectric constant. Good agreement for the charge densities for $n=3-8$ calculated using the Thomas-Fermi and self-consistent band models was found when values of $\epsilon=3.4$ and 3.0 were used, respectively.

---

*Present address: Exxon Research & Engineering, Linden, N.J. 07036.

[1] J. E. Fischer and T. E. Thompson, Phys. Today 31 (7), 36 (1977).

[2] *Proceedings of the International Conference on Layered Materials and Intercalates, Nijmegen, Netherlands, 1979* [Physica (Utrecht) 99B, 383 (1980)].

[3] *Proceedings of the Second International Conference on Intercalation Compounds of Graphite, Provincetown, Mass., 1980* [J. Synth. Met. (in press)].

[4] S. A. Safran and D. R. Hamann, Phys. Rev. Lett. 42, 1410 (1979); Physica (Utrecht) 99B, 469 (1980).

[5] S. A. Safran in Ref. 3.

[6] W. Metz and D. Hohlwein, Carbon 13, 87 (1975).

[7] S. A. Safran, Phys. Rev. Lett. 44, 937 (1980).

[8] P. Bak and J. Von Boehm, Phys. Rev. B 21, 5297 (1980).

[9] J. Von Boehm and P. Bak, Phys. Rev. Lett. 44, 122 (1978).

[10] M. E. Fisher and W. Selke, Phys. Rev. Lett. 44, 1502 (1980).

[11] L. Pietronero, S. Strässler, H. R. Zeller, and M. J. Rice, Phys. Rev. Lett. 41, 763 (1978); Solid State Commun. 30, 399 (1979).

[12] S. A. Safran and D. R. Hamann, Phys. Rev. 22, 606 (1980).

[13] G. Dresselhaus, S. Shayegan, T. Chien, and S. Y. Leung in Ref. 3.

[14] H. Suematsu, S. Tanuma, and K. Higuchi, Physica (Utrecht) 99B, 420 (1980).

[15] E. Mendez, T. C. Chieu, N. Kambe, and M. S. Dresselhaus, Solid State Commun. 33, 837 (1980).

[16] S. Tanuma, Y. Iye, O. Takahashi, and Y. Koike in Ref. 3.

[17] F. Batallan, I. Rosenman, and C. Simon in Ref. 3.

[18] R. S. Markiewicz, H. Hart, L. Interrante, and J. S. Kasper in Ref. 3.

[19] J. Blinowski, N. Hau, C. Rigaux, J. P. Vicren, R. Le Toullec, G. Furdin, A. Herold, and C. Melin, J. Phys. (Paris) 41, 47 (1980), *ibid.* 41, 667 (1980).

[20] P. C. Eklund, R. S. Smith, and V. R. K. Murthy in Ref. 3.

[21] J. J. Ritsko and E. Mele in Ref. 3; Phys. Rev. Lett. 43, 68 (1979).

[22]D. M. Hwang, S. A. Solin, M. Utlaut, and M. S. Isaacson in Ref. 3; Physica (Utrecht) 99B, 435 (1980).
[23]N. A. W. Holzwarth, Phys. Rev. B 21, 3665 (1980).
[24]M. S. Dresselhaus, G. Dresselhaus, and J. E. Fischer, Phys. Rev. B 15, 3180 (1977).
[25]L. Johnson and G. Dresselhaus, Phys. Rev. B 7, 2275 (1973).
[26]T. Ohno, K. Nakao, and H. Kamimura, J. Phys. Soc. Jpn. 47, 1125 (1979).
[27]D. DiVincenzo, N. A. W. Holzwarth, and S. Rabii in Ref. 3; Physica (Utrecht) 99B, 406 (1980).
[28]N. A. W. Holzwarth, S. Rabii, and L. A. Girifalco, Phys. Rev. B 18, 5190 (1978).
[29]H. J. Monkhorst and J. D. Pack, Phys. Rev. B 13, 5188 (1974).
[30]Since the changes in the energy levels due to c-axis hopping are (i) different for a continuum (pure graphite) and a discrete number of graphite layers (ii) affected by the potential due to charge transfer, we have considered only the in-plane dispersion in the Thomas-Fermi calculation, in contrast to Ref. (11). The quantum-mechanical band calculation presented here shows that c-axis hopping and the nonhomogeneous c-axis potential should be considered on the same footing. For a discussion of the value of $\epsilon = 3.4$ used for the Thomas-Fermi calculation, as compared with $\epsilon = 3$ used for the band calculation, see Appendix B.
[31]S. Aronson, F. J. Salzano, and D. Bellafiore, J. Chem. Phys. 49, 434 (1968).
[32]A. Herold, in *Intercalated Layered Materials*, edited by F. Levy, (D. Reidel, Dodrecht, Holland, 1979), p. 321.
[33]B. Carton and A. Herold, Bull. Soc. Chim. Fr. 4, 1340 (1972).
[34]P. L. Greenway, G. Harbeke, F. Bassani, and E. Tosatti, Phys. Rev. 178, 1340 (1969).
[35]M. Zanini, D. Grubisic, and J. E. Fischer, Phys. Status Solidi B 90, 151 (1978).
[36]H. Venghaus, Phys. Status Solidi B 71, 609 (1975).
[37]R. K. Nesbet, Phys. Rev. A 16, 1 (1977).
[38]S. Ergun, J. B. Yasinsky, and J. R. Townsend, Carbon 5, 403 (1967).